SYNTHESIS AND CHARACTERIZATION OF IRON-BASED MAGNETIC MICRO- AND NANOSPHERES

O. Corona[1]*, G. Quercia[2], A. Balza[1]

[1] PDVSA Intevep, S.A., Centro de Investigación y Desarrollo, Los Teques, República Bolivariana de Venezuela.
[2] Trican Well Service Ltd., R&D Center, Calgary, Canada

*Corresponding author, E-mail: coronao@pdvsa.com, (+58) 212 3306788.

Recibido: Octubre 2015. Aprobado: Mayo 2016.
Publicado: Mayo 2016.

ABSTRACT

The present study aims to produce and characterize magnetic iron oxide spheres on a micro - and nanoscale. Based on the process of spheroidization by flame, an industrial ferruginous laterite was used as a precursor. The micro- and nanospheres produced were magnetically separated and classified. The composition, microstructure and magnetic behavior of iron-based micro- and nanospheres were characterized by XRD, SEM, TEM and Mössbauer spectroscopy. Results showed interesting differences in terms of crystallinity for iron oxides samples, e.g. hematite, goethite, and magnetite could be identified (polycrystalline samples). Microscopy characterization gave a valuable evidence of shape homogeneity, polydispersity (microspheres up to 100 μm and nanospheres around 6 nm) and dendritic surface morphology of the particles. Magnetite dominated in iron oxide powder samples. In addition, the magnetization curves corresponded to assemblies of individual magnetic particles with mutual dipolar interactions.

Keywords: Iron-based materials; flame spheroidization; iron microspheres; iron nanospheres.

SÍNTESIS Y CARACTERIZACIÓN DE MICRO- Y NANOESFERAS MAGNÉTICAS DE ÓXIDOS DE HIERRO

RESUMEN

El presente estudio trata sobre la producción y caracterización de micro- y nanoesferas magnéticas de óxidos de hierro. Se utilizó un material ferruginoso para su esferoidización por el método de la llama. Las micro- y nanoesferas producidas fueron separadas mecánica y magnéticamente. Los materiales preparados fueron caracterizados por DRX, MEB, MET y espectroscopía Mössbauer, en términos de su composición, microestructura y comportamiento magnético. Los resultados mostraron interesantes diferencias en términos de la cristalinidad de la muestras de óxidos de hierro, pudiéndose identificar hematita, goethita y magnetita (muestras policristalinas). La caracterización por microscopía aportó evidencia valiosa de la morfología y polidispersidad de las partículas (microesferas de hasta 100 μm y nanoesferas con tamaño promedio de 6 nm) , así como arreglos dendríticos en las superficies de las mismas. Adicionalmente, se determinó la presencia mayoritaria de magnetita en todas las muestras. Las curvas de magnetización se corresponden con ensamblajes de partículas magnéticas individuales con interacciones dipolares.

Palabras claves: Materiales ferruginosos; esferoidización por llama; microesferas; nanoesferas.

INTRODUCTION

The study of new materials can be oriented in two directions: smart materials whose response is proportional to external stimuli; and nanomaterials, that have a specifically designed microscopic structure [1]. Ceramic microspheres are inorganic materials composed of finely dispersed vitreous, crystalline or pseudo-amorphous spherical particles. Due to their particular combination of physical and morphological properties (i.e. controlled particle size, density, compressive strength and insulating performance), ceramic microspheres are used in a wide variety of applications (Budov, 1994). On the other hand, magnetic micro- and nanospheres have attracted great attention due to their interesting properties and potential applications in electronics, optoelectronics, lubricants and fluids.

Magnetic fluids exhibit a special quality; they can be tailored to respond proportionally to magnetic stimuli in a desired manner. Magnetorheological fluids are those composed of ferromagnetic micro- or nanoparticles. For most of fluids, viscosity varies with temperature but in the case of magnetorheological fluids, the viscosity is easily controllable by applying an external magnetic field. Thus, a gel formation could be artificially generated and controlled in presence of a variable magnetic field [3, 4].

The present study aims to produce and characterize magnetic iron oxide spheres on a micro and nanoscale, and its potential application in the oil and gas industry. In this regard, two niches of application have been identified: drilling fluids and oilwell cementing. The rheological control of these areas is critical during the oilwell-construction process.

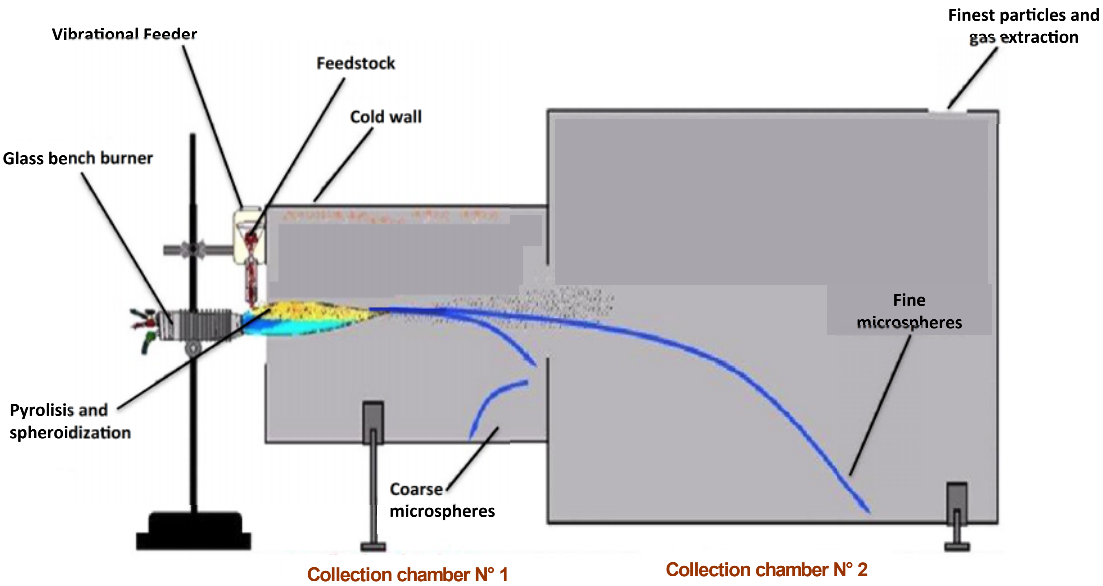

Fig. 1. Spheroidization chamber [5]

MATERIALS AND METHODS

An industrial ferruginous laterite (Granzón Menito, S.A, Venezuela) was used as raw material. The production of magnetic iron oxide spheres on a micro and nanoscale was carried out through the spheroidization process by the flame method [5]. Dry ground starting material (ball milled for 8 h; average sized < 44 μm and sieve 325) was injected into a natural gas-oxygen burner (0.6:0.6 m^3/h gas: oxygen flow ratio), promoting the partial pyrolysis and spheroidization of the raw material. Microspheres were collected on the bottom of the chambers (MIC1: material collected in the chamber 1 and MIC2: material collected in the chamber 2) and nanospheres (NanoFe) were deposited on the top (by vapor deposition on the colder wall). The composition, microstructure and magnetic behavior of all materials were characterized by X-ray diffraction (XRD diffractometer, PANalytical X´Pert Pro 40 mA and 45 KV), field emission scanning electron microscopy and energy dispersive X-ray spectroscopy (SEM-EDS, FEI Quanta FEG250-EDAX), high-resolution transmission electron microscope (HRTEM, Titan-300 kV on a copper grid) and ^{57}Fe Mössbauer spectroscopy (Transmission geometry, ^{57}Co source in a Rh matrix, a driving unit running in the triangular symmetric mode for velocity and a multichannel analyzer from Wissel Instruments).

RESULTS AND DISCUSSION

Composition and microstructural characterization

The raw material was characterized by SEM-EDS analysis. Figure 2 (a and b) and the embedded table gave evidence of mainly iron oxides (clearer contrast of particles in Figure 2-a). Additionally, the dark contrast of particles in Figure 2-a showed content of silicon oxides. The size distribution of the material was highly heterogeneous, varying from a few to 100 µm.

Figure 3 shows the XRD pattern of the ferruginous laterite, where crystalline phases, mainly composed by quartz, hematite and goethite, among others, can be identified.

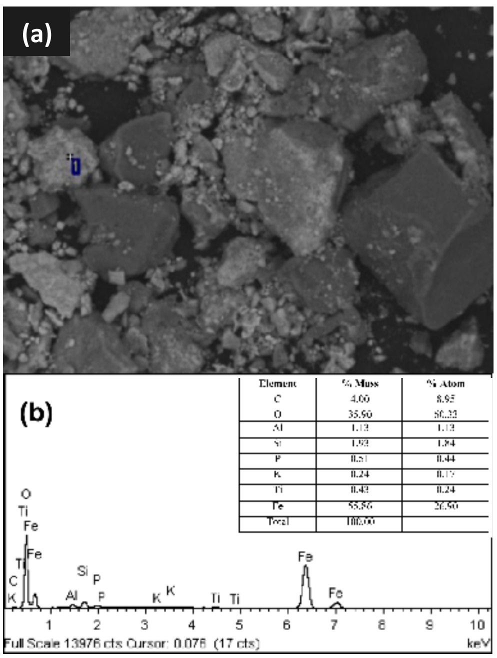

Element	% Mass	% Atom
C	4.00	8.95
O	35.90	60.33
Al	1.13	1.13
Si	1.93	1.84
P	0.51	0.44
K	0.24	0.17
Ti	0.43	0.24
Fe	55.56	26.90
Total	100.00	

Fig. 2. SEM-EDS analysis of ferruginous laterite.

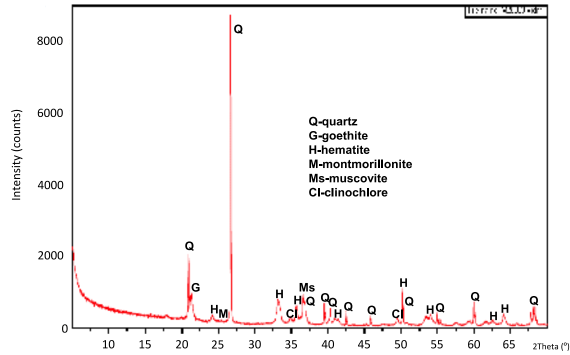

Fig. 3. XRD pattern of ferruginous laterite.

The SEM images in Figure 4 and the EDS compositional analysis (Figure 5) showed the presence of iron oxide microspheres, mainly magnetite (Fe_3O_4). Figure 6 shows the XRD pattern of microspheres, confirming the reduction of crystallinity and formation of new phases due to the high temperatures used in the spheroidization process. Typical SiO_2, Fe_2O_3-hematite and Fe_3O_4-magnetite peaks could be seen.

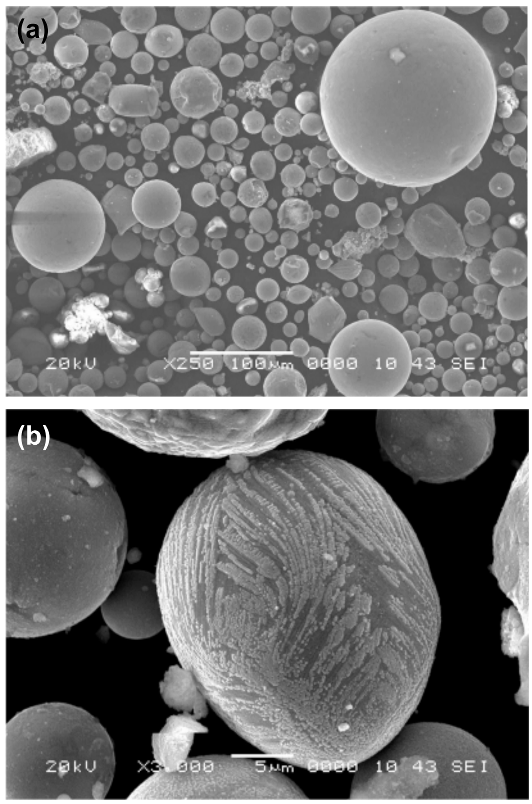

Fig. 4. SEM images of microspheres (a) Detail (100 µm), high spheroidization and (b) detail at 5 µm, dendrite surface structure.

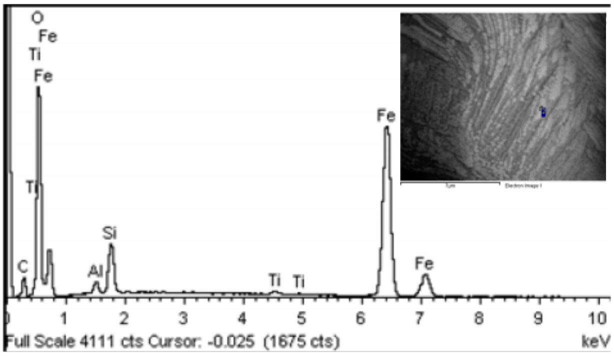

Fig. 5. EDS compositional analysis of magnetic microspheres.

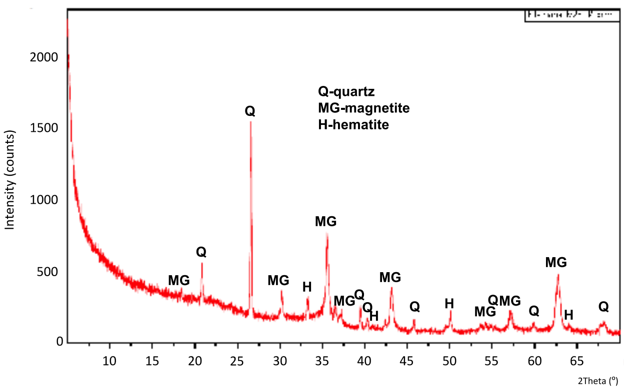

Fig. 6. XRD pattern of iron-based microspheres.

Table 1. EDS compositional analysis of iron oxide nanoparticles.

Element	% Mass	% Atom
C	4.00	8.95
O	40.90	60.33
Si	0.64	1.84
P	0.51	0.44
K	0.24	0.17
Ti	0.43	0.24
Fe	60.86	28.90
Total	100.00	

Iron-based nanospheres were characterized by HRTEM. In Figure 7, iron oxide nanoparticles with 6 nm in average size and with well-defined atomic order can be observed. EDS analysis (Table 1) gave evidence that nano-aggregates were mainly composed of iron oxides (Fe_2O_3 and Fe_3O_4). It was possible to identify SiO_2-quartz, γ-Fe_2O_3-maghemite and Fe_3O_4-magnetite peaks in the XRD pattern (Figure 8), despite lower intensity and wider peaks due to nanometric particle size.

Magnetic characterization

The results obtained from ^{57}Fe Mössbauer spectroscopy and magnetic hysteresis measurements for ferruginous laterite, iron-based microspheres and nanoparticles are shown in this section [6,7].

In Figure 9, the room temperature six-lined Mössbauer subspectrum for ferruginous laterite corresponding to hematite (Fe_2O_3) as well as a complex subspectrum for superparamagnetic goethite (FeO(OH)) can be observed. At 77 K, the superparamagnetic goethite subspectrum is clearly resolved as a six-lined spectrum for goethite (Figure 10).

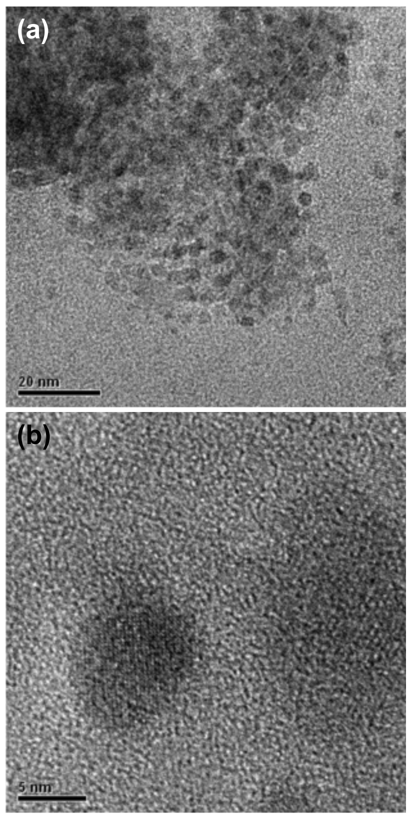

Fig. 7. HRTEM images of nanospheres. (a) Detail at 20 nm, iron oxide nanoparticles and (b) detail at 5 nm.

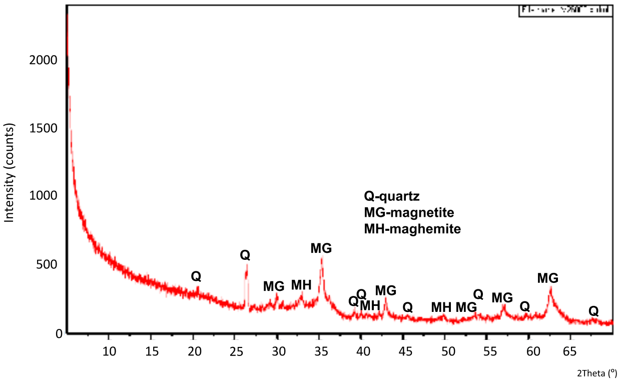

Fig. 8. XRD pattern of iron-based nanospheres.

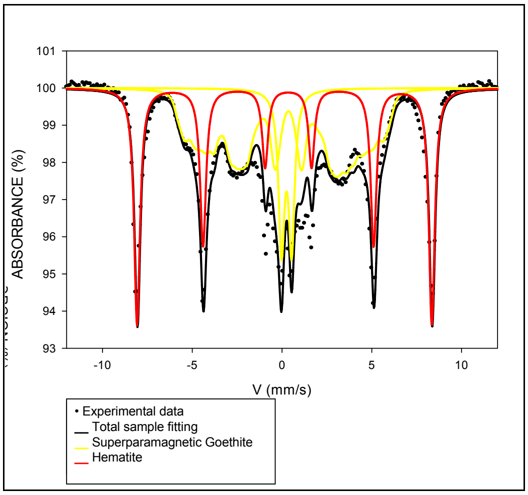

	IS (mm/s)	QS (mm/s)	B_{hyp} (T)	%
Hematite	0.38	0.22	51.0	38

Fig. 9. Mössbauer spectra of laterite sample at room temperature.

The room temperature Mössbauer experiment on the magnetic microspheres sample showed a hematite subspectrum, a Fe^{2+} doublet that probably corresponds to ferrosilicates, two magnetite subspectra and a singlet assigned to superparamagnetic magnetite (Figure 11). The magnetite percentage calculated was approximately 65%, from the sum of the two subspectra, and superparamagnetic magnetite was approximately 12%.

The Mössbauer spectroscopy results for iron-based nanoparticles also revealed the same sort and number of signals shown by the magnetic microspheres, except that the amounts of iron species changed (Figure 12). The total magnetite in the sample was 48% and the superparamagnetic magnetite increased to 38%.

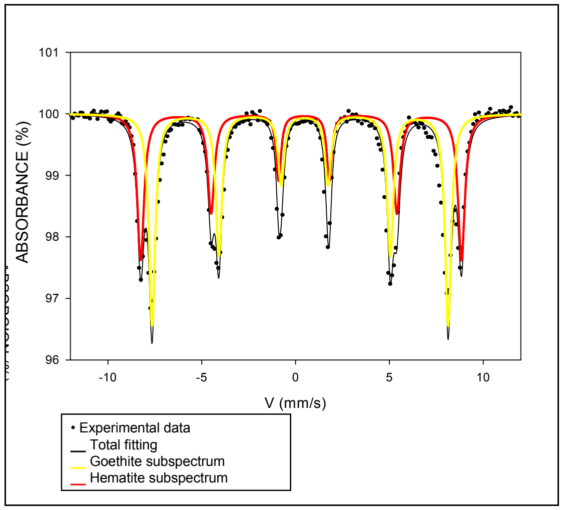

	IS (mm/s)	QS (mm/s)	B_{hyp} (T)	%
Goethite	0.47	0.24	49.0	57
Hematite	0.48	0.15	53.1	43

Fig. 10. Mössbauer spectra of laterite sample at 77 K.

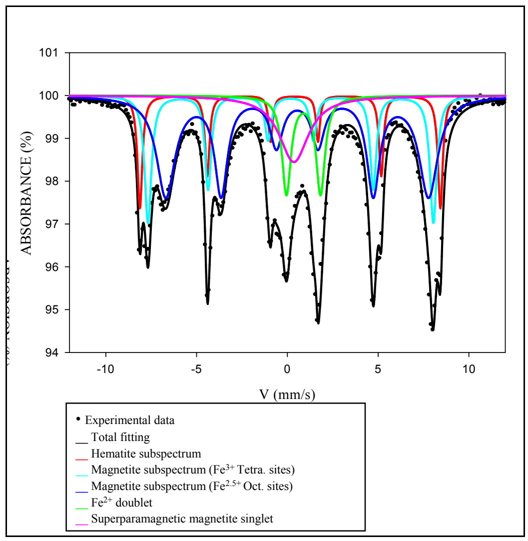

	IS (mm/s)	QS (mm/s)	B_{hyp} (T)	%
Hematite	0.38	0.23	51.4	13
Fe^{3+} Tetra.	0.29	0.00	48.8	21
$Fe^{2.5+}$ Oct.	0.65	0.00	44.9	44
Fe^{2+}	0.99	1.88	00.0	10
Singlet	0.47	0.00	00.0	12

Fig. 11. Mössbauer spectra of iron-based microspheres.

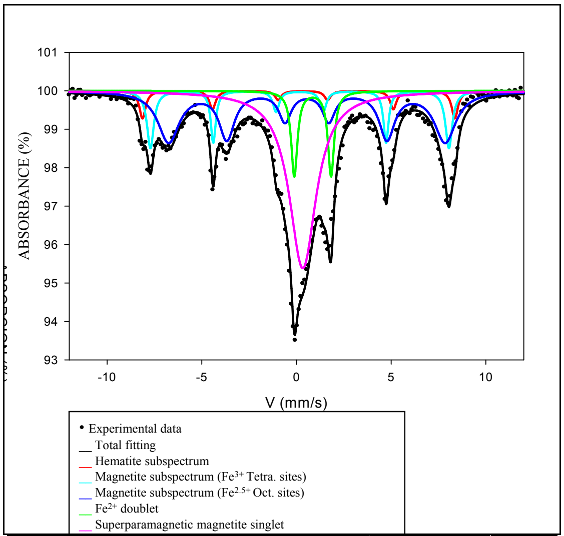

	IS (mm/s)	QS (mm/s)	Bhyp (T)	%
Hematite	0.34	0.22	51.4	5
Fe^{3+} Tetra.	0.28	0.00	48.9	13
$Fe^{2.5+}$ Oct.	0.66	0.00	45.3	35
Fe^{2+}	0.97	1.94	00.0	9
Singlet	0.44	0.00	00.0	38

Fig. 12. Mössbauer spectra of iron oxide nanoparticles.

Figure 13 summarizes the magnetic hysteresis behavior of all the samples, where M is defined as the magnetization per mass unit (emu/g: cgs units) and H is the magnetic field applied (Oe: Oersted). It can be seen that the magnetization for laterite is close to zero and no hysteresis is observed. This behavior is explained by the presence of antiferromagnetic compounds in the sample, mainly hematite and goethite. In contrast, the iron-based microspheres collected from both chambers (MIC1 and MIC2) are composed of magnetite and so have much higher magnetization values as well as hysteresis loops typical of ferromagnetic materials. The NanoFe collected on the cold wall show a lower hysteresis loop than the microspheres and this response is due to the greater portion of small particles, < 10 nm. Both microspheres and nanoparticles showed that reaching the saturation state (M_S) at 2 kOe was not possible. Higher hysteresis values lead to a better response to an external magnetic field, promoting the alignment of the magnetic spins in the material.

It is remarkable that despite the presence of superparamagnetic particles, determined by Mössbauer spectroscopy, these could not be significantly observed in the hysteresis measurements, perhaps because of the low amounts of superparamagnetic species in the bulk in comparison with ferromagnetic particles, which control the general magnetic properties. However, in MIC1 sample, it was observed that the coercive field is approximately to zero, which is an evidence of superparamagnetic behavior, possibly due to the presence of nanometric iron oxide arrangement on the surface of microspheres. Multi domain magnetic materials usually show low coercivity and remanence because of the magnetization is associated with simple energetic processes in low magnetic fields. In contrast, for single domain magnetic materials the magnetization is a process energetically costly, resulting in high coercivity and remanence.

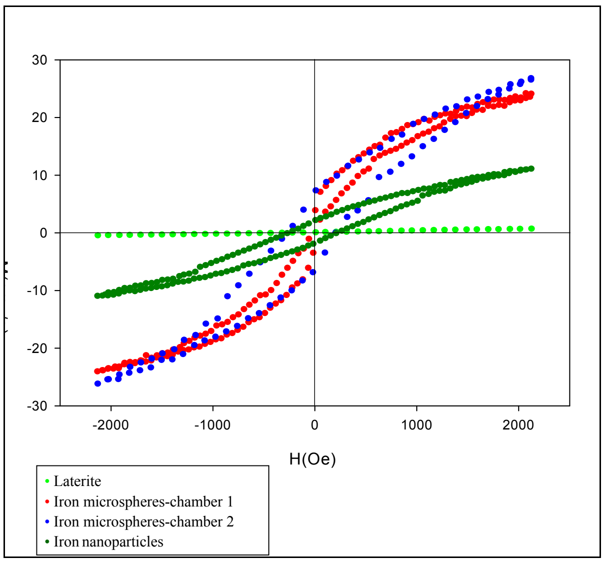

Fig. 13. Hysteresis measurements of samples.

Additionally, the Table 2 summarizes the magnetic measurements of iron oxides samples (M_R: Remanence; M_S: Saturation; H_C: Coercive field).

Table 2. Magnetic results of iron-based micro- and nanospheres

Sample	M_R (emu/g)	M_S (emu/g)	H_C (Oe)
MIC1	4.0	25.0	~ 0
MIC2	7.5	27.5	250
NanoFe	2.5	11.5	200

CONCLUSIONS

In this article it is reported the production of iron micro- and nanoparticles from an inexpensive industrial material and an efficient and scalable method.

In terms of composition and microstructure, interesting differences in development of crystallinity for iron oxides samples, e.g. hematite, goethite, and magnetite could be identified. Microscopy characterization gave a valuable evidence of shape homogeneity, polydispersity and surface morphology of the particles.

Magnetite dominated in iron oxide powder samples. In general, the magnetization curves corresponded to assemblies of individual magnetic particles with mutual dipolar interactions, separated by SiO_2 phases.

The ferromagnetic materials have a great potential for their use in magnetorheological applications because of their behavior as soft magnetic materials; hence they are easily magnetized and demagnetized.

ACKNOWLEDGEMENT

Authors want to thank to the Advanced Materials Department (CIQA) and the Physics Department (UCV) for the valuable collaboration.

REFERENCES

[1] Mesquida C.D., Lässig J.L. (2012) “Introducción a los fluidos magnetoreológicos con aplicaciones en ingeniería” *Revista Interamericana de Ingeniería Mecánica.* Vol. 16, Nº 1, Pages 27-36.

[2] Budov V. V. (1994) “Hollow glass microspheres. use, properties and technology (Review)” *Glass and Ceramics*. Vol. 51, issue 7-8, Pages 230-235.

[3] Mazlan S.A., Issa A., Chowdhury H.A., Olabi A.G. (2009) “Magnetic circuit design for squeeze mode experiments on magneorheological fluids” *Material & Desing*. Vol. 3, issue 6, Pages 1985-1993.

[4] Olabi A.G., Grunwald A. (2007) “Desing and application of magnetorheological fluid” *Material & Desing*. Vol. 28, issue 10, Pages 2658-2664.

[5] Poirier T., Quercia G. (2014) “Formation of hollow vitreous and semi-crystalline microspheres in slag flame spraying” *Ceramics International*. Vol. 41, issue 1, Pages 369–377.

[6] Murad E., 1988. “Properties and behavior of iron oxides as determined by Mössbauer spectroscopy” In: Stucki J.W., Goodman B.A., Schwertmann U. (Eds.), *Iron in Soils and Clay Minerals*. D. Reidel Publishing Company, Dordrecht, Pages 309–350.

[7] Santana G. P., Fabris J. D., Goulart A. T., Santana D. P. (2001) “Magnetite and its transformation to hematite in a soil derived from steatite” *Revista Brasileira de Ciencia do Solo*. Vol. 25, Pages 33–42.